Bulletin of the Seismological Society of America, Vol. 102, No. 1, pp. 42–52, February 2012, doi: 10.1785/0120110083

Rytov Series Approximation for Rough Surface Scattering

by Geng-Xin Yu and Li-Yun Fu

Abstract A Rytov series approximation for rough surface scattering is presented for an analytical description of the close relation of topographic statistics and topographic scattering. The Rytov series approximation is not subject to the stringent restrictions that apply to the Born series approximation. Numerical calculations of the Rytov series approximation are conducted for several benchmark models. Comparisons with the full-waveform numerical solution and the Born series approximation are made for all examples to investigate the ranges of validity of the Rytov series approximation. The first-order Rytov approximation ignores multiple scatterings between any two surface points. In general, it has been considered valid for the large-scale roughness components. The high-order Rytov approximation accounts for multiple scattering between surface points and, therefore, becomes a realistic method for multiscale surfaces. Tests with the Gaussian/semicircular convex topographies and two randomly rough topographies show that the Rytov series approximation improves the Born series approximation in both amplitude and phase. For the two sharp edges in the semicircular convexity model, the fourth-order Rytov approximation is required to account for strong wave fluctuations. For general rough surfaces without infinite gradients and extremely large surface heights, the second-order Rytov approximation might be sufficient to guarantee the accuracy of rough surface scattering.

Introduction

Topography has a significant influence on seismic data recorded at the surface. A thorough understanding of topographic scattering effects would be of obvious value to data interpretation of ground motion and regional phases. A great deal of effort has been directed to studying topographic scattering effects during the past several decades (e.g., Bouchon, 1973; Sánchez-Sesma and Campillo, 1993; Bouchon *et al.*, 1996; Cao *et al.*, 2004; Zhou and Chen, 2006a, 2008; Mogi and Kawakami, 2007). Bouchon (1973) estimated the effects of irregular surfaces using the time-domain extension of the Aki–Larner method (Aki and Larner, 1970). Sánchez-Sesma and Campillo (1993) evaluated topographic amplification for relatively simply topography. Bouchon *et al.* (1996) gave a comprehensive review of studies of the topographic scattering effects on seismic waves. They conclude that the topographic scattering is an important source of seismic coda and amplification of ground motion. Cao *et al.* (2004) investigated the scattering from various topographies for an incident *SH* wave and evaluated the accuracy, stability, and computational efficiency of three methods: the Aki–Larner method (Aki and Larner, 1970), the Bouchon–Campillo method (Bouchon, 1985; Campillo and Bouchon, 1985), and a global generalized reflection/transmission matrices method (Chen, 1990, 1995, 1996). Zhou and Chen (2006a) studied the relationship between the scales of topography and the frequency of the incident wave by using an efficient local discrete wavenumber method (Zhou and Chen, 2006b). They then extended this method to investigate the influences of the topography on the propagation of Rayleigh waves (Zhou and Chen, 2008). Mogi and Kawakami (2007) investigated the excitation process of complicated seismic responses induced by irregular ground surfaces, using detailed analyses to demonstrate that the complicated waveforms of seismic responses are caused by the arrivals of scattered waves.

Various approximations, such as perturbation theory, the Kirchhoff approximation, and the Born series method, have been widely used to model rough surface scattering (e.g., Gilbert and Knopoff, 1960; Kennett, 1972; Hudson *et al.*, 1973; Snieder, 1986). These approximation methods are comparatively simple to implement with limited validity. Most of the approximation solutions assume that the surface height should be small compared with the wavelength of an incident wave. Additional important restriction required for the validity of some approximation methods is the small surface slope. Fu (2005) summarized several approximation methods that can be used analytically to study rough surface scattering with different limited regions of validity. Numerical experiments show that the Rytov approximation gives a more accurate evaluation of rough surface scattering than does the Kirchhoff solution for most of cases (Fu, 2005; Hu *et al.*, 2009). The results also indicate that the Rytov approximation is not subject to the stringent restrictions that

apply to the Kirchhoff approximation. On the basis of these facts, it is of interest to develop the Rytov series approximation for rough surface scattering.

The Rytov approximation has been widely used in wave propagation, scattering, and diffraction tomography (Chernov, 1960; Ishimaru, 1978; Devaney, 1981, 1982, 1984; Slaney *et al.*, 1984; Wu and Toksöz, 1987; Lo *et al.*, 1988; Huang *et al.*, 1999; Tsihrintzis and Devaney, 2000). Its domain of validity, as well as its advantages and disadvantages, have been extensively explored and compared with those of the Born approximation. For instance, Mueller *et al.* (1979) and Kaveh *et al.* (1979, 1982) compared the Born and Rytov approximations in diffraction tomography based on numerical and laboratory experiments, which demonstrated that the Rytov approximation has a wider range of validity in both of the imaging frequency range and the imaged object size. Oristaglio (1985) compared the accuracy of the Born and Rytov approximations for the interface problem and concluded that the Rytov approximation to the transmitted field is more accurate than the Born approximation. Rajan and Frisk (1989) compared the Born and Rytov approximations in solving inverse backscattering problems, and pointed out that the Rytov method is less sensitive to the reference sound speed in the inversion. Rather than applying it to volume heterogeneities, as was done in the previous studies, the Rytov approximation is applied to rough topographies in this study.

A Rytov series approximation is presented in this article for analytically describing rough surface scattering. This method ignores the effects of small phase angle variation, leading to relatively simple analytical expressions for scattered field amplitudes. With this article, we will establish the validity of the method at seismic frequencies through comparisons with the full-waveform numerical solution obtained by solving a boundary integral equation using the boundary-element method (BEM; Fu and Wu, 2001). We particularly focus on designing benchmark problems to evaluate the range of validity of the Rytov series approximation. Two types of benchmark tests, a deterministic test and a statistical test, will be used for rough surface scattering in this study. The former give a topographic irregularity in terms of the surface height and the surface slope. It is fundamental to both the numerical and approximation approaches that the regions of validity be quantified in terms of the surface height and the surface slope relative to incident wavelength. The key for the deterministic test is to design a suitable benchmark geometrical model. The statistical test is based on $k\sigma$, kl, and kd for randomly rough surfaces, where k is the wavenumber, σ is the surface root-mean-square (rms) height, l is the surface correlation length, and d is the propagation distance.

First, two topographies with Gaussian and semicircular convexities of curvature radius a are used as benchmark models for the deterministic test. The accuracy of the Rytov series approximation for scattering is examined through comparison with the full-waveform BEM solutions for different ratios of curvature radius to incident wavelength (i.e., dimensionless frequency) at different incident angles. Second, randomly rough surfaces with different degrees of Gaussian-type roughness are used as benchmark models for statistical tests. We design the large-scale and small-scale randomly topographies to evaluate the Rytov series approximation. Comparisons with the Born series approximation are made for both the deterministic test and statistical tests to demonstrate superior performance of the Rytov series approximation.

Method

Boundary Integral Equation

The scattering problem to be addressed is illustrated in Figure 1. Consider 2D steady-state SH-wave incidence on a rough free surface S in a half-space. Displacements of SH waves satisfy the Helmholtz equation:

$$\nabla^2 u(\mathbf{r}) + k_0^2 u(\mathbf{r}) = 0, \tag{1}$$

where $u(\mathbf{r})$ is the displacement at location $\mathbf{r}$ on S, $k_0 = \omega/v_0$ is the wavenumber with frequency ω and wave velocity v_0, and ∇^2 is the Laplacian operator.

Based on the representation theorem (Aki and Richards, 1980), the antiplane displacement $u(\mathbf{r})$ at location $\mathbf{r}$, resulting from an incident field $u^I(\mathbf{r})$ to the rough surface with the traction-free condition, satisfied the boundary integral equation

$$u^I(\mathbf{r}) - \int_S u(\mathbf{r}') \frac{\partial G(\mathbf{r}, \mathbf{r}')}{\partial n} d\mathbf{r}' = C(\mathbf{r}) u(\mathbf{r}). \tag{2}$$

The incident harmonic plane wave is assumed as $u^I(\mathbf{r}) = \exp(i\mathbf{k}_0 \cdot \mathbf{r})$, with $\mathbf{k}_0 = (k_0 \sin\theta_0, -k_0 \cos\theta_0)$ and θ_0 being the incident angle measured from the vertical. In the presence of a point source located at $\mathbf{r}_0(x_0, z_0)$, it can be expressed by $u^I(\mathbf{r}) = s(\omega) G(\mathbf{r}, \mathbf{r}_0)$, where $s(\omega)$ is the source spectrum. The Green's function, $G(\mathbf{r}, \mathbf{r}')$, is given by $G(\mathbf{r}, \mathbf{r}') = e^{ik_0|\mathbf{r}-\mathbf{r}'|}/(4\pi|\mathbf{r}-\mathbf{r}'|)$ for 3D problems (Aki and Richards, 1980) and by $G(\mathbf{r}, \mathbf{r}') = iH_0^{(1)}(k_0|\mathbf{r}-\mathbf{r}'|)/4$ for 2D problems (Aki and Richards, 1980), where $i = \sqrt{-1}$ and $H_0^{(1)}$ denotes the Hankel function. The coefficient $C(\mathbf{r})$ is equal either to 0.5 for $\mathbf{r} \in S$ or to 1.0 for the location $\mathbf{r}$ below the surface, and $\partial/\partial n$ denotes differentiation with respect to the outward normal of the surface. Equation (2) is a Fredholm integral equation of the second

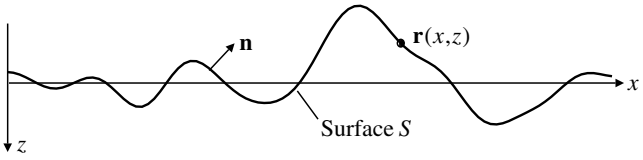

Figure 1. Configuration of the problem considered.

kind. The existence of its solution is guaranteed by the classical Fredholm theory.

Numerical Discretization of Boundary Integral Equations

The collocation method has been widely used for numerical solutions of all types of integral equations. We discretize the free surface S into L boundary elements denoted by S_e ($e = 1, 2, \ldots, L$). The total node number is N. In the collocation method, interpolation shape functions Φ are used so that the variables $\mathbf{r}$ and u are approximated by the linear combination of their nodal values over an element S_e defined geometrically between the node I_1 and I_2; for instance,

$$u(\xi) = \sum_{l=I_1}^{I_2} u(\mathbf{r}_l)\Phi_l(\xi), \tag{3}$$

where ξ denotes the local coordinate of an element.

Equation (2) can be written in operator form

$$f(\mathbf{r}_j) - Hu(\mathbf{r}_j) = 0, \qquad j = 1, 2, \ldots, N, \tag{4}$$

where f is the incident field and H is the boundary integral operator. The integrals of H can be computed over each element as

$$h_{jk} = \sum_{e=1}^{L}\sum_{l=I_1}^{I_2}\left[\int_{S_e}\frac{\partial}{\partial n}G(\mathbf{r}_j, \mathbf{r}'(\xi))\Phi_l(\xi)d\mathbf{r}'(\xi)\right]\delta_{lk} + C(\mathbf{r}_j)\delta_{jk}, \tag{5}$$

where δ_{lk} and δ_{jk} are the Kronecker delta functions, and the Gaussian integration algorithm is used to numerically evaluate these integrals. In this study, the full-waveform BEM solution is used as an exact solution for comparisons with Rytov series approximation method. The computation program of the BEM has been tested by dimensionless frequency responses of a semicircular convex topography (Fu, 2005) through comparison with the solutions by Sánchez-Sesma and Campillo (1991).

Rytov Series Approximation

Based on the superior performance of the Rytov approximation to rough surface scattering, we formulate the Rytov series approximation in this section. The Kirchhoff solution to large-scale topographic roughness is restricted by small fluctuations in amplitude and phase in the resulting wave field; that is, the phase fluctuation $\Delta\phi$ and the amplitude fluctuation ΔA, caused by topographic roughness, satisfy $\Delta\phi \ll 1$ and $\Delta A/A_0 \ll 1$, where A_0 is the amplitude of the incident field. The Rytov approximation is not subject to the stringent restrictions.

Letting $u(\mathbf{r})/u^I(\mathbf{r}) = e^{\Delta\phi(\mathbf{r})}$, then equation (2) becomes

$$C(\mathbf{r})u^I(\mathbf{r})e^{\Delta\phi(\mathbf{r})} = u^I(\mathbf{r}) - \int_S u^I(\mathbf{r}')e^{\Delta\phi(\mathbf{r}')}\frac{\partial G(\mathbf{r}, \mathbf{r}')}{\partial n}d\mathbf{r}'. \tag{6}$$

The Rytov approximation requires a small $\nabla(\Delta\phi(\mathbf{r}))$. Therefore, it is a kind of small angle approximation. Generally speaking, for large-scale topographic roughness, the Rytov approximation gives a more accurate evaluation of rough surface scattering than does the Kirchhoff solution but at the cost of an extra treatment of transformation from the wave fields $\phi(\mathbf{r})$ to $u(\mathbf{r})$, which may cause inconvenience for analytical studies of random surface scattering.

To extend the Rytov approximation, the quantity $e^{\Delta\phi(\mathbf{r})}$ in equation (6) is expanded as a Taylor series; that is,

$$e^{\Delta\phi(\mathbf{r})} = 1 + \Delta\phi(\mathbf{r}) + \frac{[\Delta\phi(\mathbf{r})]^2}{2} + \frac{[\Delta\phi(\mathbf{r})]^3}{6} + \cdots + \frac{[\Delta\phi(\mathbf{r})]^n}{n!}. \tag{7}$$

For the first-order approximation, equation (6) can be written as

$$C(\mathbf{r})u^I(\mathbf{r})[1 + \Delta\phi(\mathbf{r})] = u^I(\mathbf{r}) - \int_S u^I(\mathbf{r}')[1 + \Delta\phi(\mathbf{r}')]\frac{\partial G(\mathbf{r}, \mathbf{r}')}{\partial n}d\mathbf{r}'. \tag{8}$$

Assuming $\psi(\mathbf{r}) = u^I(\mathbf{r})\Delta\phi(\mathbf{r})$, and $\int_S u^I(\mathbf{r}')\Delta\phi(\mathbf{r}')\frac{\partial G(\mathbf{r},\mathbf{r}')}{\partial n}d\mathbf{r}' = 0$ in that $\Delta\phi \ll 1$, then we obtain

$$C(\mathbf{r})\psi_1(\mathbf{r}) = [1 - C(\mathbf{r})]u^I(\mathbf{r}) - \int_S u^I(\mathbf{r}')\frac{\partial G(\mathbf{r}, \mathbf{r}')}{\partial n}d\mathbf{r}'. \tag{9}$$

For the i-th-order approximation ($i = 2, 3, \ldots, n$), equation (6) can be written as

$$C(\mathbf{r})u^I(\mathbf{r})\left\{1 + \Delta\phi(\mathbf{r}) + \cdots + \frac{[\Delta\phi(\mathbf{r})]^i}{i!}\right\} = u^I(\mathbf{r}) - \int_S u^I(\mathbf{r}')\left\{1 + \Delta\phi(\mathbf{r}') + \cdots + \frac{[\Delta\phi(\mathbf{r}')]^i}{i!}\right\} \times \frac{\partial G(\mathbf{r}, \mathbf{r}')}{\partial n}d\mathbf{r}'. \tag{10}$$

Similarly, considering $\int_S u^I(\mathbf{r}')\frac{[\Delta\phi(\mathbf{r}')]^i}{i!}\frac{\partial G(\mathbf{r},\mathbf{r}')}{\partial n}d\mathbf{r}' = 0$, we obtain

$$C(\mathbf{r})\psi_i(\mathbf{r}) = \left\{[1 - C(\mathbf{r})]u^I(\mathbf{r}) - \int_S u_{i-1}(\mathbf{r}')\frac{\partial G(\mathbf{r}, \mathbf{r}')}{\partial n}d\mathbf{r}'\right\} \Big/ L_{i-1}(\mathbf{r}), \tag{11}$$

where

$$u_{i-1}(\mathbf{r}') = u^I(\mathbf{r}')\left\{1 + \sum_{j=1}^{i-1} \frac{[\Delta\phi_{i-1}(\mathbf{r}')]^j}{j!}\right\}$$

and $$\mathrm{L}_{i-1}(\mathbf{r}) = 1 + \sum_{\mathrm{j}=1}^{\mathrm{i}-1} \frac{[\Delta\phi_{i-1}(\mathbf{r})]^{\mathrm{j}}}{(\mathrm{j}+1)!}.$$

Then the solution to equation (6) by the Rytov series can be written as

$$\begin{aligned} C(\mathbf{r})\psi_1(\mathbf{r}) &= [1 - C(\mathbf{r})]u^I(\mathbf{r}) - \textstyle\int_S u^I(\mathbf{r}')\frac{\partial G(\mathbf{r},\mathbf{r}')}{\partial n}d\mathbf{r}' \\ C(\mathbf{r})\psi_2(\mathbf{r}) &= \left\{[1 - C(\mathbf{r})]u^I(\mathbf{r}) - \textstyle\int_S u_1(\mathbf{r}')\frac{\partial G(\mathbf{r},\mathbf{r}')}{\partial n}d\mathbf{r}'\right\} \Big/ L_1(\mathbf{r}) \\ &\vdots \\ C(\mathbf{r})\psi_n(\mathbf{r}) &= \left\{[1 - C(\mathbf{r})]u^I(\mathbf{r}) - \textstyle\int_S u_{n-1}(\mathbf{r}')\frac{\partial G(\mathbf{r},\mathbf{r}')}{\partial n}d\mathbf{r}'\right\} \Big/ L_{n-1}(\mathbf{r}). \end{aligned} \tag{12}$$

Because $u(\mathbf{r})$ and $\partial G(\mathbf{r},\mathbf{r}')/\partial n$ are continuous, convergence of equation (12) is guaranteed when

$$\max \int_S \left|\frac{\partial G(\mathbf{r},\mathbf{r}')}{\partial n}\left\{1 + \sum_{j=1}^{i-1}\frac{[\Delta\phi_{i-1}(\mathbf{r}')]^j}{j!}\right\}\right| d\mathbf{r}' < 1,$$

which strongly depends on the surface height, the surface slope, and the wavelength of the incident wave. Alternatively, we define

$$\mathbf{K}_{i-1}u = \int [\partial G(\mathbf{r},\mathbf{r}')/\partial n]\{1 + \sum_{j=1}^{i-1}\frac{[\Delta\phi_{i-1}(\mathbf{r}')]^j}{j!}\}u^I(\mathbf{r}')d\mathbf{r}'$$

to cast equation (12) in the concise form

$$\begin{aligned} C\psi_1 &= (1 - C - \mathbf{K}_0)u^I \\ C\psi_2 &= (1 - C - \mathbf{K}_1)u^I/L_1 \\ &\vdots \\ C\psi_n &= (1 - C - \mathbf{K}_{n-1})u^I/L_{n-1}, \end{aligned} \tag{13}$$

and the convergence condition becomes $q(\mathbf{K}) < 1$ (the spectral radius of $\mathbf{K}$ less than one).

The first-order Rytov approximation accounts for the single scattering between the observation point $\mathbf{r}$ and the surface point $\mathbf{r}'$, whereas the second-order Rytov approximation accounts for one more term: single scattering between two surface points ($\mathbf{r}'$ and $\mathbf{r}''$). Therefore, the high-order Rytov approximation considers multiple scattering between surface points.

Numerical Examples

Gaussian and semicircular convex topographies are typical structural units on the Earth's surface. These surface structures trap strong multiple scatterings within the hill for a limited time, making the models a typical benchmark problem for the Rytov series approximation to multiple scattering from rough surfaces. The statistical test using randomly rough surfaces with large-scale and small-scale roughness is important for applications of the Rytov series approximation to simulate regional phases. We calculate dimensionless frequency responses to these benchmark topographies for different angles of *SH*-wave incidence with comparison to the full-waveform BEM numerical simulation. It is of interest to compare the present method with the Born series approximation, which, as an iterative numerical technique, has been used for rough surface scattering and has previously undergone investigation of its validity (Fu, 2005). To make the comparison clearer, the rms error E defined as

$$E = \sqrt{\frac{\sum_{i=1}^{N}(x_i' - x_i)^2}{N}}$$

is calculated for all the examples, where x' represents the approximate solution, x represents the full-waveform BEM solution, and N is the total node number.

Deterministic Tests with Gaussian and Semicircular Convex Topographies

A semicircular convexity of radius a (Fig. 2a) is selected for validation tests because of its full scales in both the surface height $h(x)$ (from 0.0 to a) and the slope $\nabla h(x)$ (from

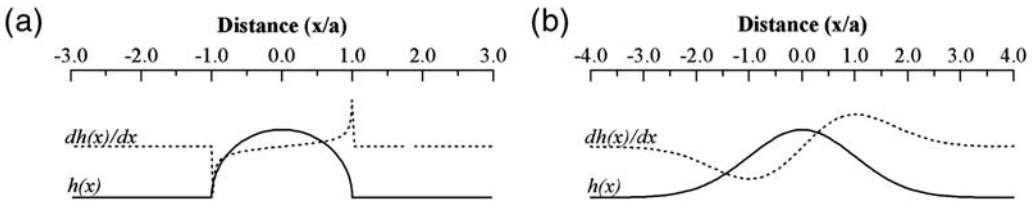

Figure 2. (a) Semicircular and (b) Gaussian convex topographies and their surface slopes.

0.0 to $\pi/2$ given by the local surface tangent at x) that make the model an ideal benchmark problem. The two sharp edges at $x = \pm a$ in the semicircular convexity model provide a crucial target to validate various numerical methods. The model introduces two extreme cases: smooth slope but large height at $x = 0$ and small height but sharp slope at $x = \pm a$, both possibly beyond the regions of validity of the low-order approximation. Being complementary to this benchmark model, a Gaussian convexity (Fig. 2b) is generated by $h(x) = (1/\sqrt{2\pi a})\exp(-x^2/2a^2)$. The Gaussian convexity introduces three cases for validation tests: smooth slope and small height in the initial section of the curve, sharp slope with moderate height in the middle section, and smooth slope but large height at the top section. For most cases, the semicircular and Gaussian convexities are combined to build a complete benchmark problem for deterministic tests of various numerical and analytical approaches to rough surface scattering. The dimensionless frequency for the deterministic tests can be defined as $\eta = 2a/\lambda$, where λ is the wavelength of incident waves. Harmonic plane waves with different wavelengths are incident on the topographies at different angles, and frequency responses on the topographic surface are calculated for different dimensionless frequencies.

Figures 3 and 4 show the amplitudes and the phases of the Rytov and Born series approximations to the Gaussian convex topography under vertical incident *SH* wave for different ratios of curvature radius to incident wavelength. Compared with the full-waveform BEM simulation, we see that the amplitude accuracy of both the Rytov and Born series approximations increases as the ratios increase in that the radius of curvature becomes greater than incident wavelength. The decreasing accuracy mainly flattens amplitude fluctuations rather than deteriorates amplitude relative variations. We see that the first-order Rytov approximation improves the first-order Born solution for all the ratios, both in amplitude and phase. For the second order, both the Rytov and Born approximations perform well for the Gaussian convex topography, giving an excellent agreement with the BEM solution for all the ratios.

Incidence can be far from the vertical for regional phases. Figures 5 and 6 show the comparison of the Rytov and the Born series approximations in both amplitude and phase to the Gaussian convexity under 60° incident *SH* wave for different ratios of curvature radius to incident wavelength. In Figure 5, we see that the amplitude accuracy of both the Rytov and Born series approximations decreases as the ratios increase, which is different from the case of vertical incidence. It is evident that the Rytov series approximation is better than the Born series approximation for all the ratios, especially in amplitude. Figure 7 shows the results under different angles of *SH*-wave incidence with a higher dimensionless frequency. It seems that the errors of the Born series approximation become larger with increasing incident angle, whereas the Rytov series approximation still performs well.

The Gaussian convexity is a smooth topography without sharp slopes. It is relatively simple so that the second-order Rytov and Born approximations can obtain an excellent agreement with the full-waveform BEM solution. Figures 8 and 9 compare the relative performances of the Rytov and the Born series approximation solutions to the semicircular convex topography for $\eta = 3.0$ under vertical and 30° incident *SH* waves, respectively. We see that strong amplitude fluctuations caused by the two sharp edges at $x = \pm a$ in

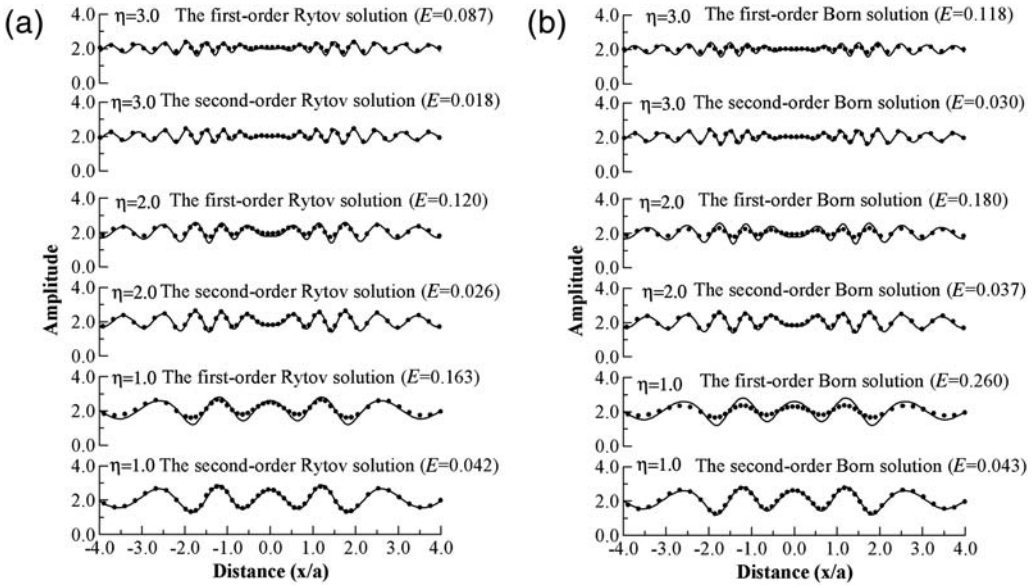

Figure 3. Comparisons of the amplitudes of the first-order and second-order Rytov and Born approximations (dotted line) to the Gaussian convex topography for various dimensionless frequencies under vertical incident *SH* wave. The solid lines denote the BEM results. Each rms error E is calculated and shown in the figure.

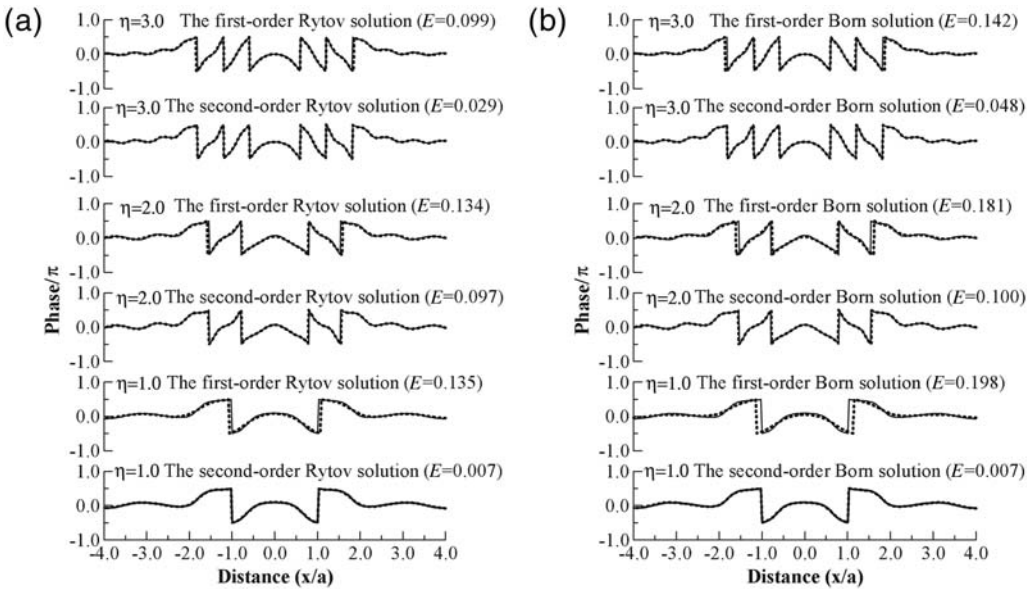

Figure 4. Comparisons of the phases of the first-order and second-order Rytov and Born approximations (dashed line) to the Gaussian convex topography for various dimensionless frequencies under vertical incident *SH* wave. The solid lines denote the BEM results. Each rms error E is calculated and shown in the figure.

the semicircular convexity destroy the performance of the low-order Rytov and the Born approximations. The low-order Rytov approximation significantly improves the low-order Born solution for the case of strong wave fluctuations, but some departures are present around the two sharp edges at $x = \pm a$, which cause strong scattering and violate the physical assumption borne in the low-order Rytov approximation.

The second-order Rytov solution performs well for $|x| < a$, but many departures occur around $|x| > a$. The third-order Rytov solution gives an excellent agreement with the BEM solution for both the areas of $|x| < a$ and $|x| > a$, whereas the third-order Born approximation presents many errors, particularly for $|x| > a$. Both of the fourth-order Rytov and Born approximations give an excellent result for the semicircular convex topography that contains infinite gradients at $x = \pm a$. For the other-than-vertical incidence shown in Figure 9, we see that the Rytov approximation performs better mainly for $x < a$ than does the Born solution for

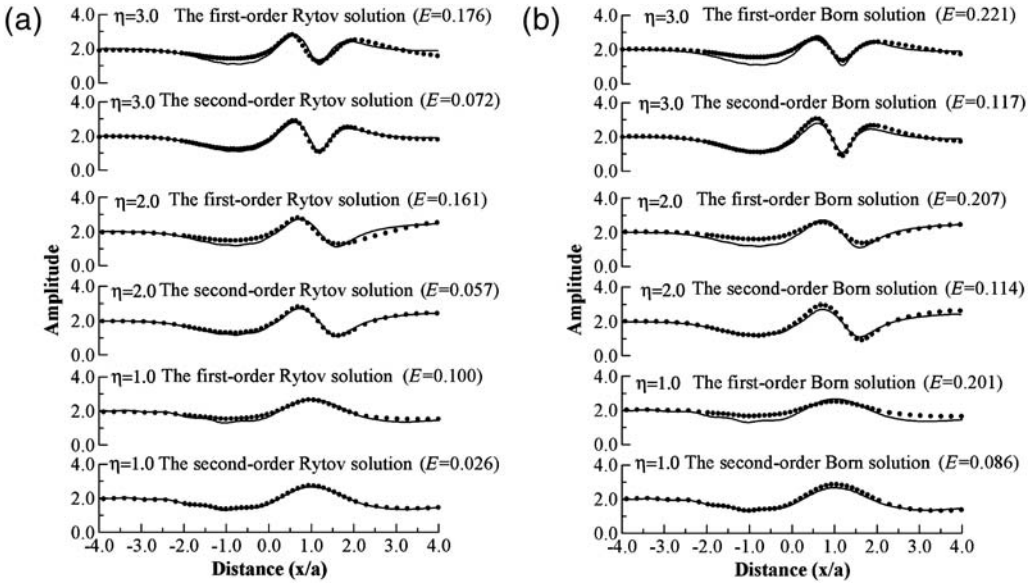

Figure 5. Comparisons of the amplitudes of the first-order and second-order Rytov and Born approximations (dotted line) to the Gaussian convex topography for various dimensionless frequencies under 60° incident *SH* wave. The solid lines denote the BEM results. Each rms error E is calculated and shown in the figure.

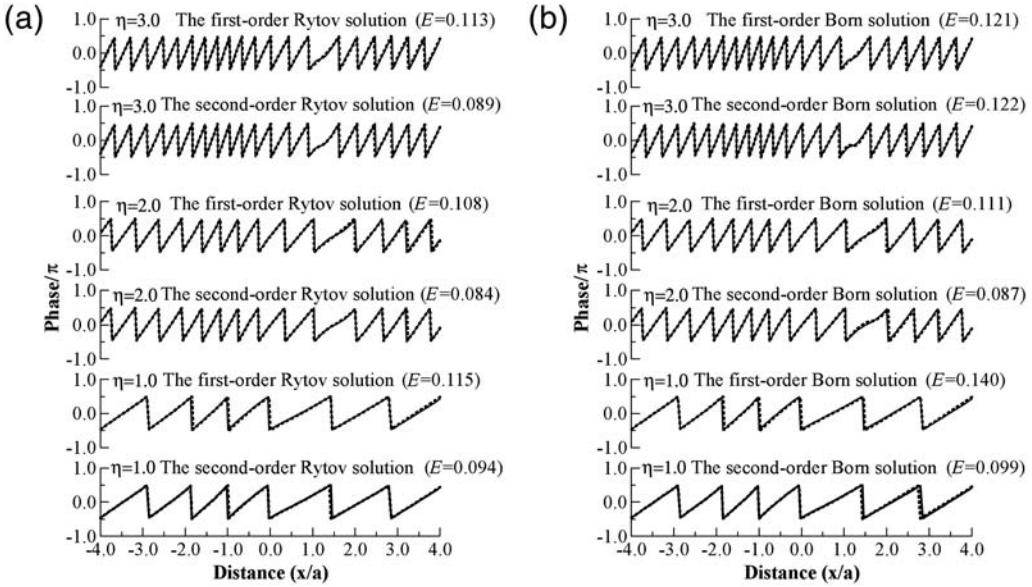

Figure 6. Comparisons of the phases of first-order and second-order Rytov and Born approximations (dashed line) to the Gaussian convex topography for various dimensionless frequencies under 60° incident *SH* wave. The solid lines denote the BEM results. Each rms error E is calculated and shown in the figure.

the second-order. The fourth-order Rytov and Born approximations have a good agreement with the full-waveform BEM solution.

Statistical Tests with Gaussian Random Topographies

The randomly rough surface can be characterized by different statistical parameters. Assuming the surface height distribution function is $h(\mathbf{r})$, where h is the height of the surface from the reference surface and $\mathbf{r}$ is the position of points on the reference surface. The rms height of the surface $h(\mathbf{r})$ is then defined as the standard deviation $\sigma = \sqrt{\langle h^2 \rangle}$, where $\langle \ldots \rangle$ denotes the process of spatial averaging across the surface. In this study, the surface is assumed to be spatially stationary and ergodic, with its $h(\mathbf{r})$ being zero mean. The roughness of the random surface height $h(\mathbf{r})$ is defined by its second moment; that is, the surface correlation function, defined as $C(\mathbf{r}) = \langle h(\mathbf{r}')h(\mathbf{r}' + \mathbf{r}) \rangle / \sigma^2$, where σ^2 is simply the variance at a lag of $\mathbf{r} = 0$ and used to normalize autocovariance $\langle h(\mathbf{r}')h(\mathbf{r}' + \mathbf{r}) \rangle$. The normalized

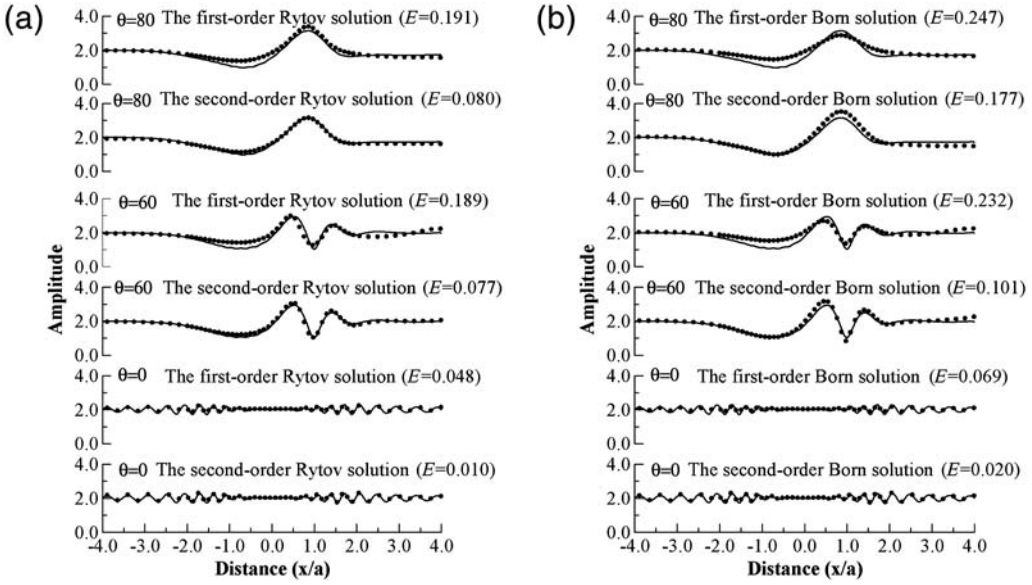

Figure 7. Comparisons of the first-order and second-order Rytov and Born approximations (dotted line) to the Gaussian convex topography with $\eta = 4.0$ under different angles of *SH*-wave incidence. The solid lines denote the BEM results. Each rms error E is calculated and shown in the figure.

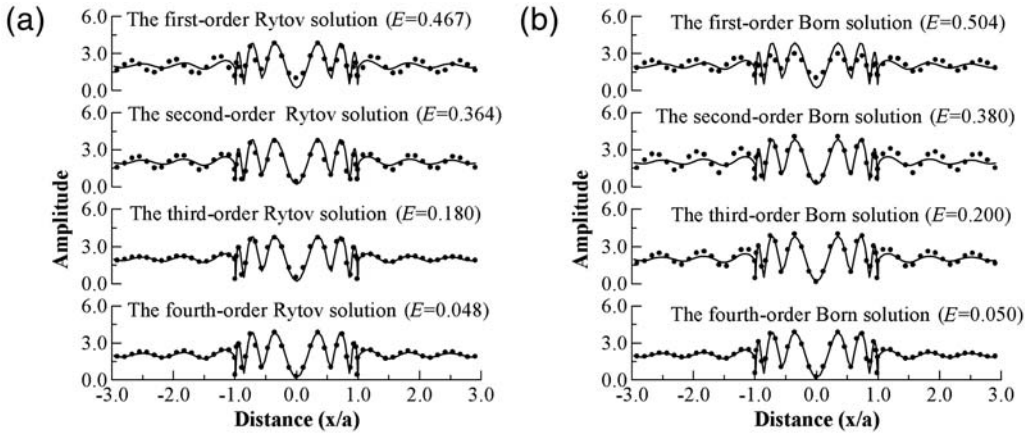

Figure 8. Comparison of Rytov and Born series approximations (dotted line) to the semicircular convex topography with $\eta = 3.0$ under vertical incident *SH* wave. The solid lines denote the BEM results. Each rms error E is calculated and shown in the figure.

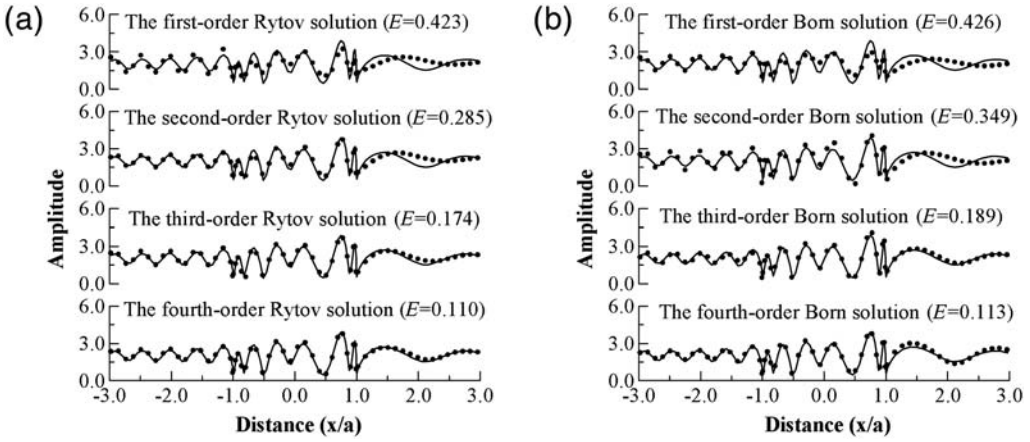

Figure 9. Comparison of Rytov and Born series approximations (dotted line) to the semicircular convex topography with $\eta = 3.0$ under 30° incident *SH* wave. The solid lines denote the BEM results. Each rms error E is calculated and shown in the figure.

autocorrelation function $C(\mathbf{r})$ has the property that $C(\mathbf{r}) = 1$ at $\mathbf{r} = 0$. It decays to zero as $\mathbf{r}$ increases to infinite. The decaying shape depends on the type of the surface; for instance, $C(\mathbf{r}) = \exp(-|\mathbf{r}|^2/l^2)$ for Gaussian roughness surfaces, with the decay rate depending on the surface correlation length l, a distance beyond which the surface profile becomes uncorrelated. Here, randomly rough surfaces with different degrees of Gaussian-type roughness are used as benchmark models for statistical tests.

The small- and large-scale topographies shown in Figure 10 are used to evaluate the Rytov series approximation. Figures 11 and 12 show different-order Rytov and Born series approximations to the small-scale topography for the cases of $kl = 3.14$ and $kl = 9.42$ under 60° incidence, demonstrating the performance of different-order approximations. It seems that the accuracies of both the Rytov and Born series approximations decrease as the kl increases. For these examples, the Rytov series approximation gives a more accurate evaluation than does the Born series approximation.

Figure 13 shows the Rytov and Born series approximations to the large-scale topography for different values of kl, compared with the full-waveform BEM numerical simulations. It can be seen that the second-order Rytov approximation gives a good agreement with the full-waveform BEM solution, improving the Born approximation mainly for the large wave fluctuations. For such rough surfaces without infinite

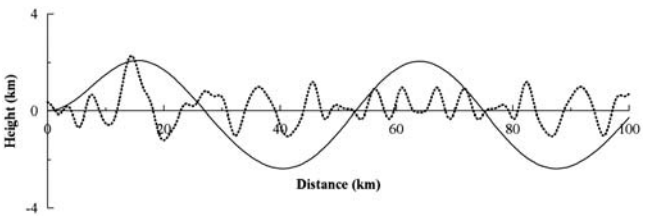

Figure 10. Two Gaussian random topographies, 100 km long at 0.25-km interval, of the same ratio ($\sigma/l = 0.3$) but with different correlation lengths, the small scale (dashed line with $l = 2.2$ km) and the large scale (solid line with $l = 22$ km).

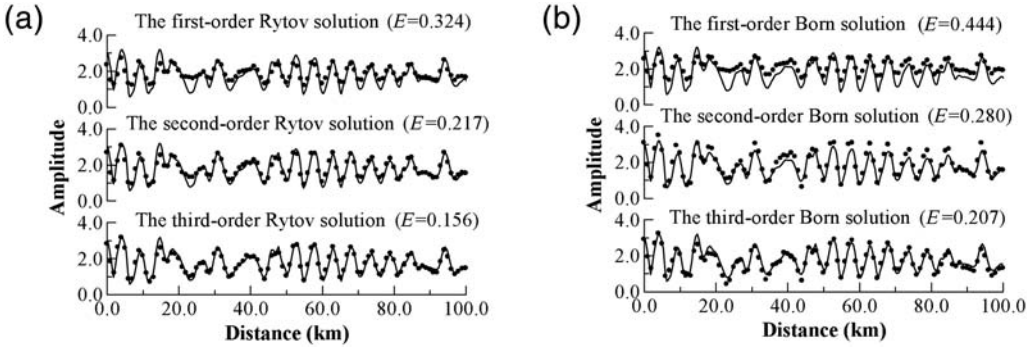

Figure 11. Comparison of Rytov and Born series approximations (dotted line) to the small-scale Gaussian roughness topography for $kl = 3.14$ under 60° incident SH wave. The solid lines denote the BEM results. Each rms error E is calculated and shown in the figure.

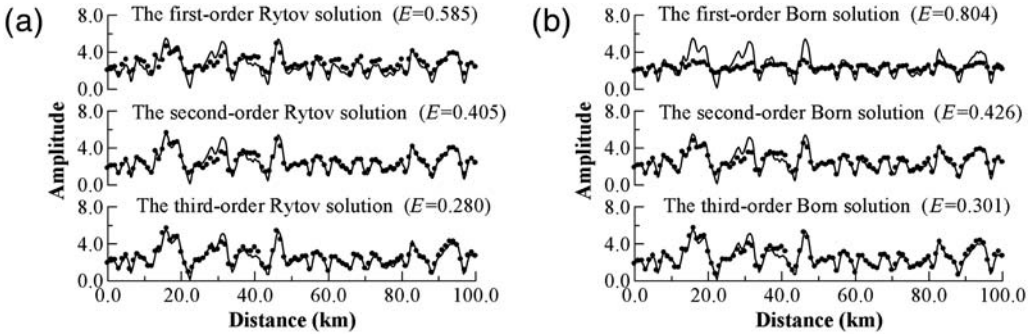

Figure 12. Comparison of Rytov and Born series approximations (dotted line) to the small-scale Gaussian roughness topography for $kl = 9.42$ under 60° incident SH wave. The solid lines denote the BEM results. Each rms error E is calculated and shown in the figure.

gradients and large surface heights, the second-order Rytov approximation might be sufficient to guarantee the accuracy of rough surface scattering.

Discussions and Conclusions

In this article, a Rytov series approximation for rough surface scattering is presented for an analytical description of the close relation of topographic statistics and topographic scattering. Two types of benchmark tests, a deterministic test and a statistical test, are used to evaluate the present method. Two topographies with Gaussian and semicircular convexities of curvature radius a are used as benchmark models for the deterministic test. Also, randomly rough surfaces with different degrees of Gaussian-type roughness are used as benchmark models for statistical tests. Comparisons with

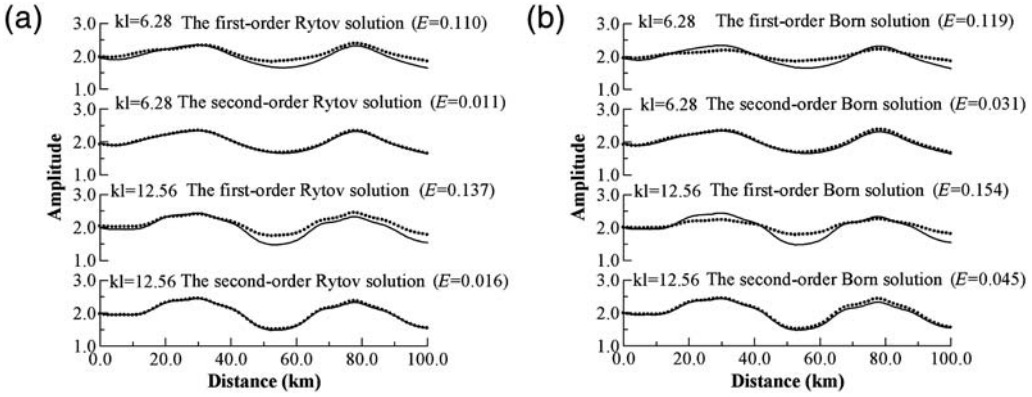

Figure 13. Comparison of Rytov and Born series approximations (dotted line) to the large-scale Gaussian roughness topography for $kl = 6.28$ and $kl = 12.56$ under 60° incident SH wave. The solid lines denote the BEM results. Each rms error E is calculated and shown in the figure.

the full-waveform numerical solution and the Born series approximation are made for all examples to investigate the ranges of validity of the Rytov series approximation.

Numerical examples demonstrate that the Rytov series approximation gives superior performance by comparison with the Born series approximation for most cases. Tests with the Gaussian/semicircular convex topographies and two randomly rough topographies show that the Rytov series approximation improves the Born series approximation in both amplitude and phase. For the two sharp edges in the semicircular convexity model, the fourth-order Rytov approximation is required to account for strong wave fluctuations. For general rough surfaces without infinite gradients and extremely large surface heights, the second-order Rytov approximation might be sufficient to guarantee the accuracy of rough surface scattering.

Data and Resources

No data were used in this article.

Acknowledgments

We thank Michel Bouchon and two anonymous reviewers for their constructive reviews and valuable comments. The research was supported by the Natural Science Foundation of China (Grant Nos. 40925013 and 41130418).

References

Aki, K., and K. L. Larner (1970). Surface motion of a layered medium having an irregular interface due to incident plane *SH* waves, *J. Geophys. Res.* **75,** no. 5, 933–954.

Aki, K., and P. G. Richards (1980). *Quantitative Seismology. Theory and Methods*, W. H. Freeman, San Francisco, 27–32.

Bouchon, M. (1973). Effect of topography on surface motion, *Bull. Seismol. Soc. Am.* **63,** 615–632.

Bouchon, M. (1985). A simple, complete numerical solution to the problem of diffraction of *SH* waves by an irregular surface, *J. Acoust. Soc. Am.* **77,** 1–5.

Bouchon, M., C. A. Schultz, and M. N. Toksöz (1996). Effect of three dimensional topography on seismic motion, *J. Geophys. Res.* **101,** 5835–5846.

Campillo, M., and M. Bouchon (1985). Synthetic *SH* seismograms in a laterally varying medium by discrete wavenumber method, *Geophys. J. Roy. Astron. Soc.* **83,** 307–317.

Cao, J., Z. X. Ge, J. Zhang, and X. F. Chen (2004). A comparative study on seismic wave methods for multilayered media with irregular interfaces, Part 1: Irregular topography problem, *Chinese J. Geophys.* **47,** no. 3, 495–503.

Chen, X. F. (1990). Seismogram synthesis for multi-layered media with irregular interfaces by global reflection/transmission matrices method. I. Theory of two-dimensional *SH* case, *Bull. Seismol. Soc. Am.* **80,** 1696–1724.

Chen, X. F. (1995). Seismogram synthesis for multi-layered media with irregular interfaces by global reflection/transmission matrices method. II. Applications for two-dimensional *SH* case, *Bull. Seismol. Soc. Am.* **85,** 1094–1106.

Chen, X. F. (1996). Seismogram synthesis for multi-layered media with irregular interfaces by the global generalized reflection/transmission matrices method, part III: Theory of 2D *P-SV* case, *Bull. Seismol. Soc. Am.* **86,** 389–405.

Chernov, L. A. (1960). *Wave Propagation in a Random Medium*, McGraw-Hill, New York, 61–66.

Devaney, A. J. (1981). Inverse-scattering theory with the Rytov approximation, *Optics Lett.* **6,** 374–376.

Devaney, A. J. (1982). A filtered back propagation algorithm for diffraction tomography, *Ultrason. Imag.* **4,** 336–350.

Devaney, A. J. (1984). Geophysical diffraction tomography, *IEEE Trans. Geosci. Remote Sens.* **22,** 3–13.

Fu, L. Y. (2005). Rough surface scattering: Comparison of various approximation theories for 2D *SH* waves, *Bull. Seismol. Soc. Am.* **95,** 646–663.

Fu, L. Y., and R. S. Wu (2001). A hybrid BE-GS method for modeling regional wave propagation, *Pure Appl. Geophys.* **158,** 1251–1277.

Gilbert, F., and L. Knopoff (1960). Seismic scattering from topographic irregularities, *J. Geophys. Res.* **65,** 3437–3444.

Hu, S. Z., L. Y. Fu, and Z. X. Yao (2009). Comparison of various approximation theories for randomly rough surface scattering, *Wave Motion* **46,** 281–292.

Huang, L. J., M. C. Fehler, P. M. Roberts, and C. C. Burch (1999). Extended local Rytov Fourier migration method, *Geophysics* **64,** 1535–1545.

Hudson, J. A., R. F. Humphryes, I. M. Mason, and V. K. Kembhavi (1973). The scattering of longitudinal elastic waves at a rough free surface, *J. Phys. Appl. Phys.* **6,** 2174–2186.

Ishimaru, A. (1978). *Wave Propagation and Scattering in Random Media*, Vol. **2**, Academic Press, New York, 349–351.

Lo, T. W., M. N. Toksöz, S. H. Xu, and R. S. Wu (1988). Ultrasonic laboratory tests of geophysical tomographic reconstruction, *Geophysics* **53,** 947–956.

Kaveh, M., R. K. Muller, and R. D. Iverson (1979). Ultrasonic tomography based on perturbation solution to the wave equation, *Comput. Graph. Image Process.* **9,** 105–116.

Kaveh, M., M. Soumekh, and R. K. Muller (1982). A comparison of Born and Rytov approximation in acoustic tomography, J. P. Powers (Editor), *Acoustical Imaging*, vol. **11**, Plenum Press, New York, 325–335.

Kennett, B. L. N. (1972). Seismic waves in laterally varying media, *Geophys. J. Roy. Astron. Soc.* **27,** 310–325.

Mogi, H., and H. Kawakami (2007). Analysis of scattered waves on ground with irregular topography using the direct boundary element method and Neumann series expansion, *Bull. Seismol. Soc. Am.* **97,** 1144–1157.

Mueller, R. K., M. Kaveh, and G. Wade (1979). Reconstructive tomography and applications to ultrasonics, *Proc. IEEE* **67,** 567–587.

Oristaglio, M. S. (1985). Accuracy of the Born and Rytov approximations for reflection and refraction at a plane interface, *J. Opt. Soc. Am.* **2,** 1987–1993.

Rajan, S. D., and G. V. Frisk (1989). A comparison between the Born and Rytov approximations for the inverse backscattering problem, *Geophysics* **54,** 864–871.

Sánchez-Sesma, F. J., and M. Campillo (1991). Diffraction of *P*, *SV* and Rayleigh waves by topographic features: A boundary integral formulation, *Bull. Seismol. Soc. Am.* **81,** 2234–2253.

Sánchez-Sesma, F. J., and M. Campillo (1993). Topographic effects for incident *P*, *SV* and Rayleigh waves, *Tectonophysics* **218,** 113–125.

Slaney, M., A. C. Kak, and L. Larsen (1984). Limitations of imaging with first-order diffraction tomography, *IEEE Trans. Microw. Theor. Tech.* **32,** 860–874.

Snieder, R. (1986). The influence of topography on the propagation and scattering of surface waves, *Phys. Earth Planet. In.* **44,** 226–241.

Tsihrintzis, G. A., and A. J. Devaney (2000). High order (nonlinear) diffraction tomography: Inversion of the Rytov series, *IEEE Trans. Inform. Theor.* **46,** 1748–1761.

Wu, R. S., and M. N. Toksöz (1987). Diffraction tomography and multisource holography applied to seismic imaging, *Geophysics* **52,** 11–25.

Zhou, H., and X. F. Chen (2006a). The study on the frequency responses of topography with different scales due to incident *SH* wave, *Chin. J. Geophys.* **49,** no. 1, 205–211.

Zhou, H., and X. F. Chen (2006b). A new approach to simulate scattering of *SH* waves by an irregular topography, *Geophys. J. Int.* **164,** no. 2, 449–459.

Zhou, H., and X. F. Chen (2008). The localized boundary integral equation —discrete wavenumber method for simulating *P-SV* waves scattering by an irregular topography, *Bull. Seismol. Soc. Am.* **98,** no. 1, 265–279.

Key Laboratory of the Earth's Deep Interior
Institute of Geology and Geophysics
Chinese Academy of Sciences
Beijing 100029
China
lfu@mail.iggcas.ac.cn

Manuscript received 21 March 2011